Romanian Reports in Physics **72**, 902 (2020)

USING TRACKER AS VIDEO ANALYSIS AND AUGMENTED REALITY TOOL FOR INVESTIGATION OF THE OSCILLATIONS FOR COUPLED PENDULA

S. TROCARU[1,2,#], C. BERLIC[1*,#], C. MIRON[1*,#], V. BARNA[1,#]

[1] University of Bucharest, Faculty of Physics, 405 Atomistilor Street, 077125, Magurele, Romania
[2] "Goethe" German College, 17 Cihoschi Street, Bucharest, Romania
[*] Corresponding authors: *cberlic@gmail.com; cmiron_2001@yahoo.com*
[#] All authors equally contributed to this work as first author.

Received July 20, 2019

Abstract. Augmented Reality (AR) allows students to overlap the reality with additional information or indirect observation through a technological device of the physics of reality. The aim of this paper is to present the use of Tracker for learning a classical study in the coupled oscillations of two coupled pendula. We show the study of the symmetric normal mode, antisymmetric normal mode and the beats phenomena for the oscillations of coupled pendula. Measurements are made by recording the experiment with a digital camera and using Tracker software, video analysis and video modeling tool to process and get information from recorded videos. With this set-up detailed comparisons can be established between theoretical calculations and measurements, focusing on several relevant concepts such as the oscillation period for the symmetrical and antisymmetrical mode, the elastic coupling spring constant and the beats period dependence on the position of the spring coupling. Consequently, the experiment based on video analysis of the experiment is used to emphasize key physical concepts, to motivate students in their exploratory work and also to stimulate autonomous investigations.

Key words: coupled pendula, Tracker software, Augmented Reality, physics education.

1. INTRODUCTION

Many authors show that experiments in the field of physics education can be projected to make use of low-cost modern electronic devices and software and thus better explain many physical phenomena. Students find the use of such devices and software as interesting and existing works exemplify their use with computer optical mouse devices [1–2], digital cameras [3–4], Arduino microcontroller [5–8], microphones [9] and computer simulations [10–12].

Augmented Reality (AR) is one of the technologies for developing interactive teaching applications in physics and it leads to novel ideas and innovative practices. These applications can be used by teachers as an additional tool for understanding the studied concepts [13–14]. The fundamental idea of augmented reality is to

encourage existing classical experiments used in Physics laboratory classes. A current practical application of augmented reality is composed of superimposing text and synthetic images on the actual picture collected by a camera [15]. Thus, digital video capture devices are increasingly being employed since they excel in technical specifications (spatial resolution and frame rate). This led to the emergence of free video analysis programs such as Tracker [16]. Tracker is a free video modeling tool built on the Open Source Physics (OSP) Java framework, developed in the Open Source Project. The features offered by Tracker include object tracking with the position, velocity and acceleration overlays and graphs, special effect filters, multiple reference frames, calibration points, line profiles for analysis of spectra and interference patterns, and dynamic particle models. The educational valence of using Tracker was emphasized in conjunction with the development of the students' conceptual thinking [17] as a solution for making physics more attractive for the learners.

Several publications present these approaches to various subjects of physics learning by means of Tracker software [18]. For example, in classical mechanics, describing simple and inexpensive experiments addressed to university and secondary levels and requiring few resources and tools associated with Tracker software can provide relevant physical parameters such as damping constants, amplitudes, frequencies [19]. Other examples include moments of inertia of fidget spinner obtained with a high precision and accuracy by using video analysis [20], moment of inertia of a cylindrical plate [21], study of the damped harmonic motion of an underwater pendulum oscillating in tap water for measuring fluid viscosity [22], experimental studies for rolling motions of a solid cylinder on soft underlays and a soft cylinder on rigid platforms [23]. The range of applications for the Tracker Video software can be easily extended to the study of electricity and magnetism experiments by employing the conversion of kinematic variables (position as a function of time) to electrical ones (voltages and currents as a function of time) [24], the comprehension of some relevant conceptual topics such as superconductor perfect diamagnetism and the difference between the Meissner effect and the Faraday one [25], the dependence of a magnetic force on the distance between permanent magnets [26].

In this paper we have used a digital camera for taking information from the real experiment for the study of the oscillations of a coupled pendula system and then to transfer the research to the augmented reality software (Tracker).

2. THEORETICAL MODEL

We show a short theoretical background of the physical behavior and mathematics behind the coupled pendula system [27–31].

Let us consider two identical pendula, each of them composed by a rod of length L and having attached a mass m to one end. The pendula are suspended at

the same height, allowed to oscillate in the vertical plane while connected by a horizontal mass-less spring of elastic constant *k*. The spring is attached to the rods at a distance *l* from the suspension points (Fig. 1).

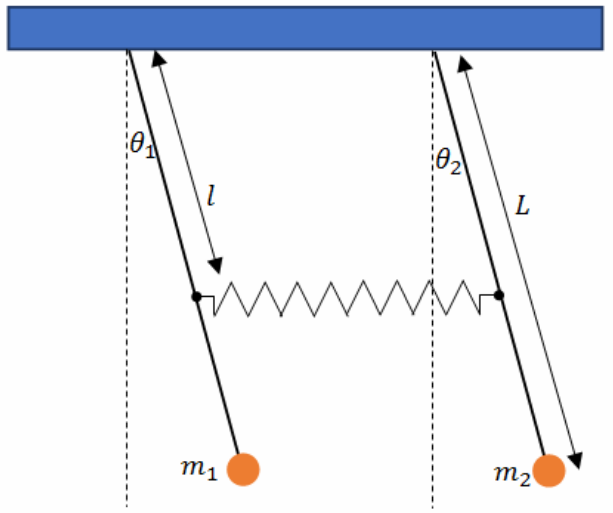

Fig. 1 – Schematic representation of the experimental setup.
The full color version may be accessed at http://www.rrp.nipne.ro.

For each pendulum we have [27–31]:

$$I_i\ddot{\theta}_i = M_i,\ i = 1,2, \tag{1}$$

with: θ_i – the angle between the rod and vertical axis; I_i –the moment of inertia of a pendulum around its suspension point. In our case $I_1 = I_2 \overset{def}{=\!=} I$; M_i – the torque exerted on each rod.

The torque on a rod around the suspension point is determined by the weight of the attached mass m and by the spring tension:

$$M_i = -M_{Gi} + M_{Ei}, \qquad i = 1,2, \tag{2}$$

where

$$M_{Gi} = mgL\sin\theta_i, \tag{3}$$

$$M_{Ei} = kxl\cos\theta_i, \tag{4}$$

with *x* being the extension of the spring.

If the deflections angles of both pendula are small, $\sin\theta_i \cong \theta_i$ and $\cos\theta_i \cong 1$ and the equation for each pendulum becomes [27–32]:

$$I\ddot{\theta}_1 = -mgL\theta_1 + kl^2\left(\theta_2 - \theta_1\right) \tag{5}$$

$$I\ddot{\theta}_2 = -mgL\theta_2 - kl^2\left(\theta_2 - \theta_1\right). \tag{6}$$

In the above relations it was assumed that $\left(\theta_2 > \theta_1\right)$ and the restoring torque on the pendula is equal in magnitude but in the opposite direction.

If we divide relations (5) and (6) by I and rearrange the terms we obtain:

$$\ddot{\theta}_1 + \left(\omega_0^2 + \Omega^2\right)\theta_1 - \Omega^2\theta_2 = 0 \tag{7}$$

$$\ddot{\theta}_2 + \left(\omega_0^2 + \Omega^2\right)\theta_2 - \Omega^2\theta_1 = 0, \tag{8}$$

with the notations:

$$\omega_0^2 = \frac{mgl}{I} \tag{9}$$

$$\Omega^2 = \frac{kl^2}{I}. \tag{10}$$

Equations (7) and (8) are a set of coupled second-order linear differential equations. These equations do not describe simple harmonic motion because of the coupling terms determined by the spring. The general solution of the system (7) and (8) is [27–32]:

$$\theta_1(t) = u_0\cos\left(\omega_S t + \varphi_u\right) + v_0\cos\left(\omega_a t + \varphi_v\right) \tag{11}$$

$$\theta_2(t) = u_0\cos\left(\omega_S t + \varphi_u\right) - v_0\cos\left(\omega_a t + \varphi_v\right), \tag{12}$$

where

$$\omega_S = \omega_0 \tag{13}$$

$$\omega_a = \sqrt{\omega_0^2 + 2\Omega^2}, \tag{14}$$

while u_0, v_0, φ_u and φ_v are constant that are determined from initial conditions.

The general solution (11) and (12) is investigated elsewhere [29, 32] and we will discuss here only the situations experimentally studied.

2.1. SYMMETRIC NORMAL MODE

The symmetric normal mode is obtained when both pendula are equally displaced in the same direction and then allowed to be free. It is obvious that, in this situation, the spring will not have any effect in the system.

In this case, the initial conditions are:

$$\theta_1(0) = \theta_2(0) = \theta_s \tag{15}$$

$$\dot{\theta}_1(0) = \dot{\theta}_2(0) = 0, \tag{16}$$

and the angular elongations of the two pendula are:

$$\theta_i(t) = \theta_s \cos \omega_s t, \quad i = 1,2. \tag{17}$$

Both pendula oscillate in phase with the same amplitude and with the same frequency, while following relation (13). This frequency is equal to the frequency of the uncoupled pendula [29].

2.2. ANTISYMMETRIC NORMAL MODE

The antisymmetric normal mode is achieved by moving the pendula with equal size and opposite direction displacements:

$$\theta_1(0) = \theta_2(0) = \theta_a \tag{18}$$

$$\dot{\theta}_1(0) = \dot{\theta}_2(0) = 0. \tag{19}$$

The angular elongations of the two pendula are:

$$\theta_1(t) = \theta_a \cos \omega_a t \tag{20}$$

$$\theta_2(t) = -\theta_a \cos \omega_a t. \tag{21}$$

Both pendula oscillate with the same amplitude and the same frequency such as in (14). The minus sign in relation (22) means that there is a permanent phase shift equal with π between the two pendula $\theta_2(t) = \theta_a \cos(\omega_a t + \pi)$.

From (14) one may notice that the frequency for this mode is higher than the frequency of the symmetric one. It is due to the fact that in the asymmetric mode the spring is stretched, increasing the forces on the pendula.

At this point we have also the linear dependence of ω_a^2 as function of l^2:

$$\omega_a^2 = \omega_0^2 + \omega_0^2 \frac{2kl^2}{mgl}. \tag{22}$$

This dependence will be checked during experiments.

2.3. BEATS

When the system is in the uncoupled mode, the amplitudes are constant and there is no energy transfer between the two pendula. For other situations, there is an energy transfer back and forward between the pendula, as it is suggested by the general solutions (11) and (12). The energy transfer is maximum when the two modes are present in equal amounts [29].

This is easy to confirm when the initial conditions are:

$$\theta_1(0) = \theta_b \tag{23}$$

$$\theta_2(0) = 0 \tag{24}$$

$$\dot{\theta}_1(0) = \dot{\theta}_2(0) = 0. \tag{25}$$

The angular elongations of the two pendula are:

$$\theta_1(t) = \theta_b \cos\frac{\omega_a - \omega_s}{2} t \cos\frac{\omega_a + \omega_s}{2} t. \tag{26}$$

$$\theta_2(t) = \theta_b \sin\frac{\omega_a - \omega_s}{2} t \sin\frac{\omega_a + \omega_s}{2} t \tag{27}$$

Considering $\omega_1 = \frac{\omega_a - \omega_s}{2}$ and $\omega_2 = \frac{\omega_a + \omega_s}{2}$ the relations (26) and (27) can be rewritten as follows:

$$\theta_1(t) = \theta_{1\max}(t)\cos\omega_2 t, \tag{28}$$

$$\theta_2(t) = \theta_{2\max}(t)\sin\omega_2 t, \tag{29}$$

where the amplitudes $\theta_{i\max}(t),\ i = 1,2$ are varying with time:

$$\theta_{1\max}(t) = \theta_b(t)\cos\omega_1 t \tag{30}$$

$$\theta_{2\max}(t) = \theta_b(t)\sin\omega_1 t. \tag{31}$$

According to [3], the equations (26) and (27) describe the superposition of two oscillations that have the beat phenomenon meaningful only if the variation in time of the amplitudes is very small by comparison with the pulsation ω_2 i.e.:

$$|\omega_a - \omega_s| << \omega_a + \omega_s. \tag{32}$$

With this assumption, the relations (13) and (14) become:

$$\omega_1 = \frac{\sqrt{\omega_0^2 + 2\Omega^2} - \omega_0}{2} \approx \omega_0 \frac{k}{2mgL} l^2 \tag{33}$$

$$\omega_2 = \frac{\sqrt{\omega_0^2 + 2\Omega^2} + \omega_0}{2} \approx \omega_0 \frac{k}{2mgL} l^2 + \omega_0. \tag{34}$$

These equations are verified within the experiment together with the assumption that real beats effect also occurs.

3. EXPERIMENTAL SET-UP AND METHOD

The experimental set-up is a Phywe system of coupled pendula represented in Fig. 2. Instead of using the provided recorder for the measurements of the vibrational period we employed digital camera to record the real movements of the pendula, the videos being afterward processed with the Tracker software.

Tracker offers the advantage of optical recognition for the position of one or more moving objects in each frame (in a recorded movie). Tracker normally uses the standard 30 Frame per Second (FPS) videos, but the frame rate can be adjusted after importing of the movie into the application. We used MPEG VX videos taken with a Sony Cyber-shot DSC-H2 camera (640 × 480 resolution and 30 FPS). The distance from the camera to the experimental device was above 2 meters.

The videos were maximum 1 minute long, enough to capture at least 20 full oscillations. By default, the allocated memory is 247 MB that can be increased to a maximum that depends on the amount of the available memory in the computer resources. The used maximum memory was 1285 MB, ensuring a reasonable processing time.

Once the movie is loaded Tracker allows making a frame by frame optical recognition of an initial pattern selected in a chosen key-frame of the loaded movie. The application identifies the frame rate of the movie and records the moment of time t of the frame and the position of the recognized pattern. For 30 FPS videos, the time resolution is 1/30 s. The objects' coordinates are recorded regarding the position of the origin of the system of coordinates chosen in the rotation point of the pendula. The time length of the analyzed fragment of the videos was chosen in such a way that we have a reasonable number of positions of the each of two objects (*i.e.* movie frames with good clarity of the image of the bodies in each frame).

Fig. 2 – Experimental set-up. The full color version may be accessed at http://www.rrp.nipne.ro.

4. DATA ANALYSIS

The data processing was performed with the data analysis tool of the Tracker software. The recorded data about the position of the bodies as function of time was used by Tracker to calculate the rotational angle of the pendula at each moment.

Both symmetrical and antisymmetrical oscillation-modes of the coupled system were analyzed from the recorded experiments, for positions of the coupling spring between 30 and 90 cm.

We used the fitting capabilities of the software, in order to find the analytical time dependence of the rotational angle. The expression for the fitting function was:

$$\theta_i = A\sin\left(Bt + C\right) + D, \tag{35}$$

where:

- the index *i* refers to the pendula, explicitly 1 for the left side body and 2 for right side one.
- *A* represents is the *angular amplitude* $\theta_{i\max}$ [rad],
- *B* represents the *angular velocity* ω [rad/s];
- C and D represents two fitting parameters needed to fit the data for the second pendulum that rotation point is not in the origin of the coordinate system. In the initial calibration, the origin of the coordinate system was set in the rotation point of the first pendulum, situated in the left side in Fig. 2.

All the time dependences for both experimental data and fitting functions of the small angles' deviations for both pendula were found sinusoidal (Fig. 3).

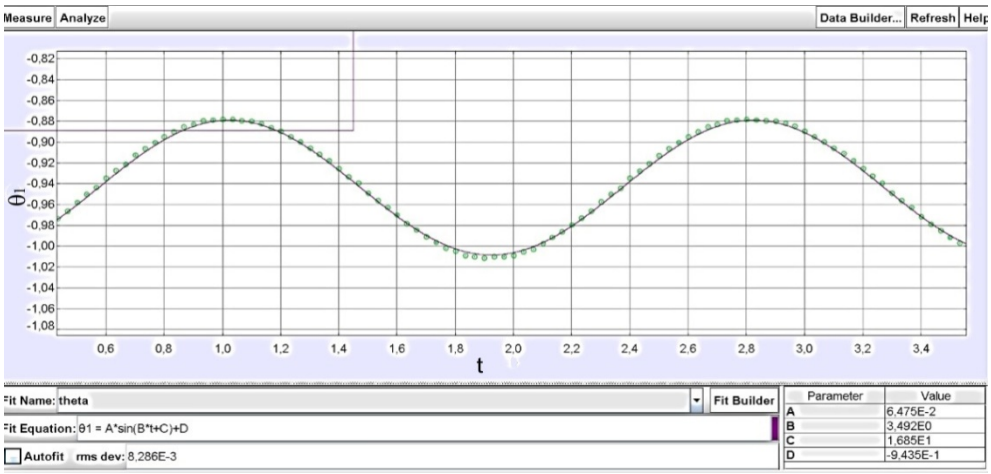

Fig. 3 – Data fitting view of the Tracker software. Experimental and fitted data for angular elongation as function of time, for one of the pendula. The full color version may be accessed at http://www.rrp.nipne.ro.

We consider that the resulting fit according to relation (35) is very good, as the calculated values of the root mean square deviation are small.

The values of angular velocities obtained from fitting data for antysimetrical and symmetrical for both pendula are put together in Table 1.

In Fig. 4, we plotted the values of ω_a^2 as function of l^2 for the antisymmetric oscillation mode. We notice that both graphs are linear as it is expected from relation (22).

Table 1

The values of angular velocities for antisymmetric ω_{ai} and symmetric ω_{si} modes for the both pendula i = 1,2

l [m]	$\omega_{a1}\left[\frac{\text{rad}}{\text{s}}\right]$	$\omega_{a2}\left[\frac{\text{rad}}{\text{s}}\right]$	$\omega_{s1}\left[\frac{\text{rad}}{\text{s}}\right]$	$\omega_{s2}\left[\frac{\text{rad}}{\text{s}}\right]$
0.305	3.231	3.243	3.155	3.155
0.400	3.306	3.308	3.156	3.154
0.496	3.382	3.384	3.157	3.155
0.610	3.490	3.489	3.156	3.156
0.697	3.584	3.588	3.159	3.159
0.793	3.701	3.696	3.154	3.154
0.898	3.826	3.811	3.153	3.154

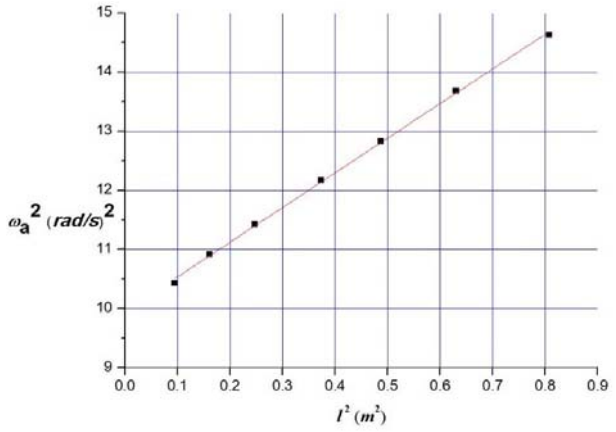

a)

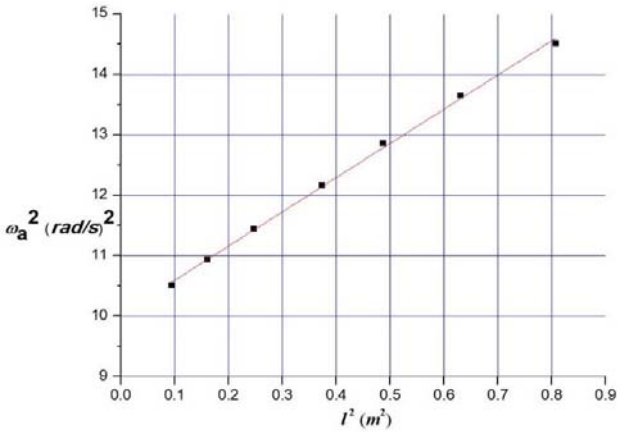

b)

Fig. 4 – Dependence of ω_a^2 as function of l^2 for pendulum 1 (a) and 2 (b) in antisymmetric oscillation mode.

The equations for the linear regression in the case of the antisymmetric oscillating pendula are:

$$\omega_{a1}^2 = 5.8649 \cdot l^2 + 9.9703 \tag{36}$$

$$\omega_{a2}^2 = 5.6618 \cdot l^2 + 10.048. \tag{37}$$

The data set for the symmetrical mode is plotted plots in Fig. 5.

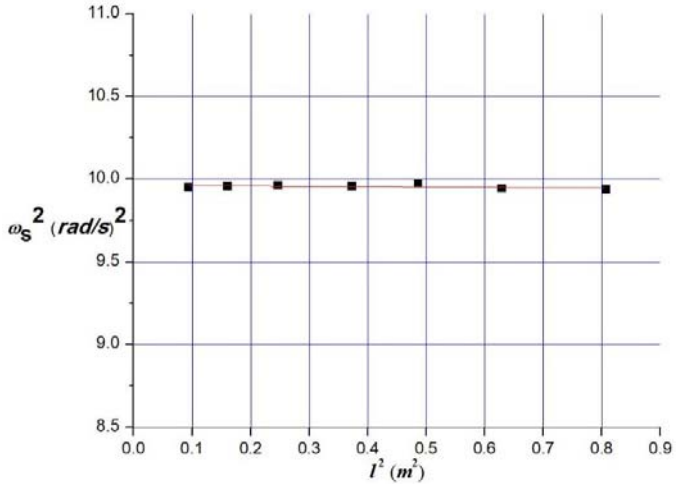

a)

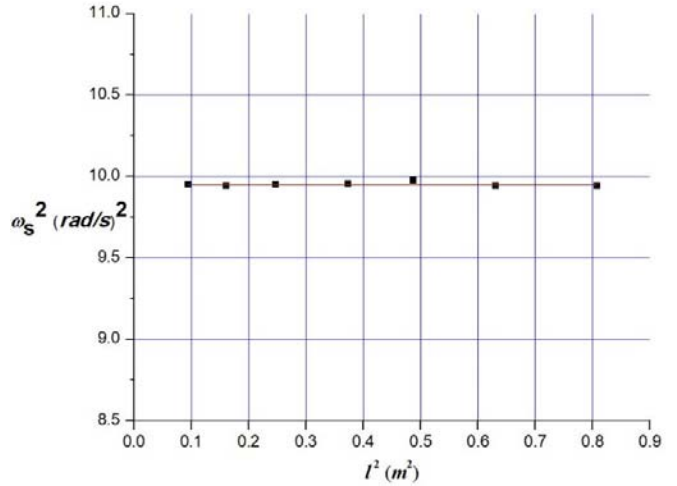

b)

Fig. 5 – Dependence of ω_s^2 as function of l^2 for pendulum 1 (a) and 2 (b) for the symmetrical oscillation mode.

The linear fit for the symmetric oscillation modes are:

$$\omega_{s1}^2 = 0.019 \cdot l^2 + 9.9665 \tag{38}$$

$$\omega_{s2}^2 = -0.0012 \cdot l^2 + 9.9563. \tag{39}$$

We notice that the lines are virtually horizontal, meaning that ω_{si}^2 is constant as it is expected from relation (13).

4.1. ESTIMATION OF FREE PENDULUM PERIOD AND THE ELASTIC CONSTANT OF THE COUPLING SPRING

The values for ω_0 in the case of both pendula are extracted from equations (36)–(39) based theoretical relations (13) and (22) and synthetized in Table 2. We may notice the very good agreement between values of ω_0 obtained for the two cases.

Table 2

ω_0 for pendulum 1 and 2 in antisymmetric and symmetric modes	$\omega_0^2 \left[\frac{\text{rad}}{\text{s}}\right]^2$	Absolute Error of ω_0^2	$\omega_0 \left[\frac{\text{rad}}{\text{s}}\right]$
Antisymmetric mode pendulum 1	9.971	0.039	3.158
Antisymmetric mode pendulum 2	10.048	0.047	3.170
Symmetric mode pendulum 1	9.966	0.009	3.157
Symmetric mode pendulum 2	9.956	0.009	3.155

Using the data in Table 1, we obtained the value for the single pendulum period:

$$T_0 = 1.984 \pm 0.200 \text{ [s]}. \tag{40}$$

The same period of oscillation was also calculated using the equation for the simple pendulum [27, 29]:

$$T_{calc} = 2\pi\sqrt{\frac{L}{g}}. \tag{41}$$

The value is:

$$T_{calc} = 2.005 \pm 0.080 \text{ [s]} \tag{42}$$

that is in relatively good agreement with the value from (39).

The value for the elastic constant of the coupling spring k may be estimated from the regression relations (36) and (37) having in mind the linear dependence of ω_a^2 on l^2 in relation (22). For the elastic constant, we get:

$$k = 2.824 \pm 0.008 \text{N/m}. \tag{43}$$

4.2. ANALYSIS OF BEATS

In order to investigate the beats phenomenon (as discussed in section 2.3.) we keep a pendulum in the position of equilibrium and the second one is deviated at a given small angle, corresponding to the initial conditions (23)–(25).We then recorded videos for different values of l and we processed them as already described before. Figure 6 illustrates the data and the fitting plot of the oscillations for pendulum 1 with $l \approx 80$ cm in beating conditions. The plot in the figure confirms the expected time dependence from equation (27).

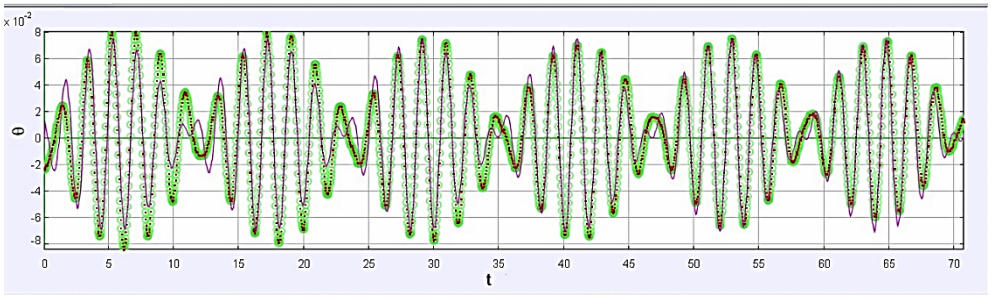

Fig. 6 – Experimental data and fitting plot of the angular elongation as function of time for one of the pendulum illustrating the beats. The full color version may be accessed at http://www.rrp.nipne.ro.

The results of the fitting data for ω_a, ω_s, ω_1 in the case of both pendula are given in Tables 3 and 4.

Table 3

Beats parameters for pendulum 1

l [m]	$\omega_a \left[\frac{\text{rad}}{\text{s}}\right]$	$\omega_s \left[\frac{\text{rad}}{\text{s}}\right]$	$\omega_1 \left[\frac{\text{rad}}{\text{s}}\right]$	$\omega_2 \left[\frac{\text{rad}}{\text{s}}\right]$
0.294	3.236	3.152	0.042	3.194
0.391	3.306	3.156	0.075	3.231
0.486	3.382	3.157	0.113	3.270
0.585	3.480	3.158	0.161	3.319
0.697	3.570	3.133	0.219	3.352
0.793	3.706	3.169	0.269	3.438

Table 4

Beats parameters for pendulum 2

l [m]	$\omega_a\left[\frac{\text{rad}}{\text{s}}\right]$	$\omega_s\left[\frac{\text{rad}}{\text{s}}\right]$	$\omega_1\left[\frac{\text{rad}}{\text{s}}\right]$	$\omega_2\left[\frac{\text{rad}}{\text{s}}\right]$
0.294	3.205	3.158	0.024	3.182
0.391	3.303	3.156	0.073	3.230
0.486	3.382	3.157	0.113	3.270
0.585	3.480	3.158	0.161	3.319
0.691	3.595	3.156	0.220	3.376
0.780	3.701	3.169	0.266	3.435

The plot of ω_1 and ω_2 as function of l^2 for the beats mode are represented in Fig. 7 and Fig. 8 respectively.

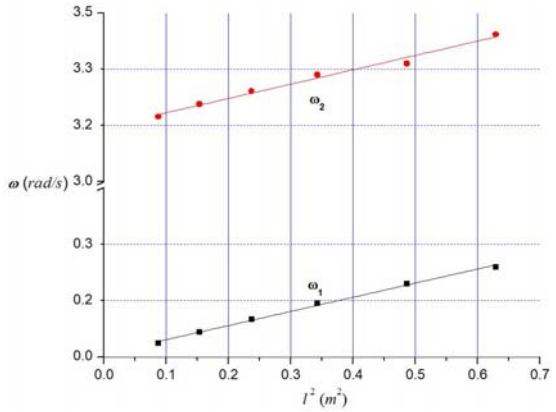

Fig. 7 – Dependence of ω_1 and ω_2 as function of l^2 for pendulum 1. For readability reasons, we broke the O*Y* axis. The full color version may be accessed at http://www.rrp.nipne.ro.

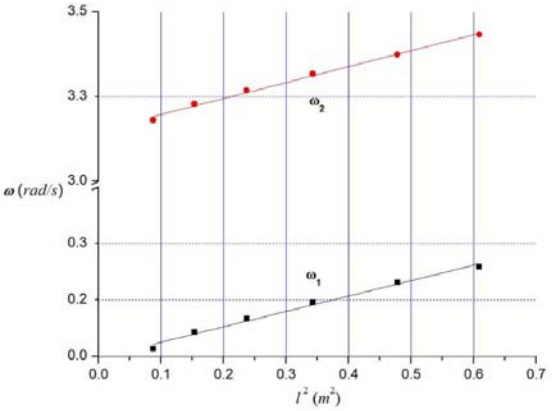

Fig. 8 – Dependence of ω_1 and ω_2 as function of l^2 for pendulum 2. For readability reasons, we broke the O*Y* axis. The full color version may be accessed at http://www.rrp.nipne.ro.

From Fig. 7 and Fig. 8, one may notice the linearity of the plotted data for both pendula, as expected from relations (33) and (34).

The value of the main pulsation of the free pendulum, ω_0, was calculated according to relation (31) from the intercept value of $\omega_2(l^2)$ regression line. Analyzing the beats, we get the estimated value for ω_0:

$$\omega_0 = (3.158 \pm 0.019)\frac{\text{rad}}{\text{s}}. \tag{44}$$

Consequently, the value of the oscillation period T_0 is:

$$T_0 = (1.989 \pm 0.040)\text{s}. \tag{45}$$

The coupling constant was obtained from relations (33) and (34) by using the slope values calculated for $\omega_1(l^2)$ and $\omega_2(l^2)$ regressions lines:

$$k = (2.749 \pm 0.038)\text{N/m}. \tag{46}$$

5. CONCLUSIONS

The values for the period T_0 obtained from the symmetric and antisymmetric oscillation modes in (40) and from the beats in relation (45) are approximately equal and in good agreement with the calculated values from the experimental setup parameters T_{calc} in relation (42).

The resolved values of the coupling spring constant are well matching with those achieved from the symmetric and antisymmetric oscillation mode in (43) and from beats in relation (46).

The values of ω_a, ω_s that were determined from direct measurements for antisymmetric and symmetric oscillation modes and summarized in Table 1 and from the beats analysis in Tables 3 and 4 confirm the assumptions made in the theoretical model:

– According to (13) and (14), the frequency for the antisymmetric mode is higher than the frequency of the symmetric one. In the asymmetric mode the spring is stretched, increasing the forces on the pendula.

– Relations (28) and (29) very well express the beats effect and the theoretical model is meaningful for analyzing the obtained graphs by means of the Tracker software.

The data found from the investigation of the coupled oscillators is in agreement with the direct determined value of k.

From the point of view of didactical approach, the overall conclusion is that Tracker is a very flexible tool, being able to analyze mechanical oscillatory motion.

The use of Tracker software on good quality experimental setup videos allows shifting the didactical focus on the analysis of the physics significance of

obtained plots and data and not spending precious time on ensuring conditions for better measurement conditions. Furthermore, the reproducibility of the experiment is automatically ensured.

In order to get suitable experimental data, the use of quite expensive laboratory equipment is required. Tracker software is a free solution and with its optical recognition capability and the versatile data tool is a great solution in performing high-quality measurements, while taking into account that superior quality videos can simply be achieved with even a regular smartphone.

REFERENCES

1. O. R. Ochoa and N. F. Kolp, Am. J. Phys. **65**, 1115–1118 (1997).
2. T. W. Ng and K. T. Ang, Am. J. Phys. **73**, 793–795 (2005).
3. J. A. Monsoriu, M. H. Giménez, J. Riera, A. Vidaurre, Eur. J. Phys. **26**, 1149–1155 (2005).
4. T. Greczylo and E. Debowska, Eur. J. Phys. **23**, 441–447 (2002).
5. B. Kos, M. Grodzicki and R. Wasielewski, Eur. J. Phys. **39**(3), 035804 (2018).
6. S. Dinu, B. Dobrica and S. Voinea, Rom. Rep. Phys. **71**, 905 (2019).
7. D. Pantazi, S. Dinu and S. Voinea, Rom. Rep. Phys. **71**, 902 (2019).
8. M. Oprea and C. Miron, Rom. Rep. Phys. **68**(4), 1621–1639 (2016).
9. E. Widiatmoko, W. Srigutomo and N. Kurniasih, Phys. Educ. **47**(6), 709 (2012).
10. B. Mihalache and C. Berlic, Rom. Rep. Phys. **70**(2), 901 (2018).
11. I. Grigore, C. Miron and E. S. Barna, Rom. Rep. Phys. **68**(2), 891–904 (2016).
12. D. Marciuc, C. Miron and E. S. Barna, Rom. Rep. Phys. **68**(4), 1603–1620 (2016).
13. F. Reyes-Aviles and C. Aviles-Cruz, Comput. Appl. Eng. Educ. **26**(3), 602–616 (2018).
14. M. P. Strzys, S. Kapp, M. Thees, P. Klein, P. Lukowicz, P. Knierim, A. Schmidt, J. Kuhn, Eur. J. Phys. **39**(3), 035703 (2018).
15. E. E. Aveleyra, D. A. Racero, G. G. Toba, *The didactic potential of AR in teaching physics*, Proceedings of 2nd IEEE World Engineering Education Conference (EDUNINE), 2018, pp. 234–236.
16. http://physlets.org/tracker/
17. P. Hockicko, L. Kristak and M. Nemec, Eur. J. Eng. Educ. **40**(2), 145–166 (2015).
18. T. Claessens, Phys. Teach. **55**(9), 558–560 (2017).
19. V. L. B. De Jesus, C. Haubrichs, A. L. De Oliveira and D. G. G. Sasaki, Eur. J. Phys. **39**(2), 025704 (2018).
20. V. L. B. De Jesus and D. G. G. Sasaki, Phys. Teach. **56**(9), 639–642 (2018).
21. T. Eadkhong, R. Rajsadorn, P. Jannual and S. Danworaphong, Eur. J. Phys. **33**(3), 615–622 (2012).
22. J. C. Leme and A. Oliveira, Phys. Teach. **55**(9), 555–557 (2017).
23. L. Vozdecký, J. Bartoš and J. Musilová, Eur. J. Phys. **35**(5), 055004 (2014).
24. P. Aguilar-Marín, M. Chavez-Bacilio and S. Jáuregui-Rosas, Eur. J. Phys. **39**(3), 035204 (2018).
25. A. Bonanno, G. Bozzo, M. Camarca and P. Sapia, Eur. J. Phys. **36**(4), 045010 (2015).
26. P. Onorato, P. Mascheretti and A. Deambrosis, Eur. J. Phys. **33**(2), 385–395 (2012).
27. A. P. French, *Newtonian Mechanics*, The M.I.T. Introductory Physics Series, W. W. Norton & Company, 1971.
28. https://www.nikhef.nl/~h73/kn1c/praktikum/phywe/LEP/Experim/1_3_25.pdf
29. A. P. French, *Vibrations and Waves*, The M.I.T. Introductory Physics Series, CBS Publishers & Distributors, 2003.
30. M. Alonso, E. J. Finn, *Fundamental University Physics*, Vol. I "Mechanics", Addison-Wesley Publishing Company, 1967.
31. J. Carlos Castro-Palacio, L. Velazquez-Abad, F. Gimenez and J. A Monsoriu, Eur. J. Phys. **34**, 737–744 (2013).
32. D. Baleanu, A. Jajarmi, and J. H. Asad, Rom. Rep. Phys. **71**(1), 103 (2019).